Popular summary of:
"The retrieval of ozone profiles from limb scatter measurements: Theory" by D. Flittner et al.

A new technique to measure the ozone vertical distribution using sunlight scattered from the Earth's limb has been proposed. The technique has the advantage of giving global coverage on a daily basis with vertical resolution of 1-3 km from the tropopause to the stratopause. This paper details an algorithm for retrieving vertical profiles of O_3 concentration using measurements of UV and visible light scattered from the limb of the atmosphere. The UV measurements provide information about the ozone profile in the upper and middle stratosphere, while only visible wavelengths are capable of probing the lower stratospheric ozone profile. Sensitivity to the underlying scene reflectance is greatly reduced by normalizing measurements at a tangent height high in the atmosphere (~55 km), and relating measurements taken at lower altitudes to this normalization point. To decrease the effect of scattering by thin aerosols/clouds that may be present in the field of view, these normalized measurements are then combined by pairing wavelengths with strong and weak ozone absorption. We conclude that limb scatter can be used to measure O_3 between 15 km and 50 km with 2-3 km vertical resolution and better than 10% accuracy.

The retrieval of ozone profiles from limb scatter measurements: Theory

D. E. Flittner and B. M. Herman
University of Arizona, Tucson, Arizona

P. K. Bhartia, R. D. McPeters, and E. Hilsenrath
Laboratory for Atmospheres, Goddard Space Flight Center, Greenbelt, Maryland

Abstract: An algorithm is presented for retrieving vertical profiles of O_3 concentration using measurements of UV and visible light scattered from the limb of the atmosphere. The UV measurements provide information about the O_3 profile in the upper and middle stratosphere, while only visible wavelengths are capable of probing the lower stratospheric O_3 profile. Sensitivity to the underlying scene reflectance is greatly reduced by normalizing measurements at a tangent height high in the atmosphere (~55 km), and relating measurements taken at lower altitudes to this normalization point. To decrease the effect of scattering by thin aerosols/clouds that may be present in the field of view, these normalized measurements are then combined by pairing wavelengths with strong and weak O_3 absorption. We conclude that limb scatter can be used to measure O_3 between 15 km and 50 km with 2-3 km vertical resolution and better than 10% accuracy.

1. Introduction

To date, the satellite based methods used to monitor the stratospheric O_3 profile have consisted primarily of nadir looking backscatter ultraviolet (buv) measurements [*Bhartia et al.,* 1996] and several different limb measurements; visible and infrared limb occultation [*Chu et al.,* 1989; *Bruhl et al.,* 1996; *Abrams et al.,* 1996], infrared limb emission [*Remsberg et al.,* 1984], and microwave limb emission [*Froidevaux et al.,* 1996]. Soon a new method, limb scatter, will be added to this list. This technique will be used by several new instruments, such as the Optical Spectrograph and Infrared Imaging System (OSIRIS), the Scanning Imaging Absorption SpectroMeter for

Atmospheric ChartographY (SCIAMACHY), and the Ozone Mapping/Profiler Suite aboard the National Polar-orbiting Operational Environmental Satellite System (OMPS/NPOESS), to monitor O_3 well into the 21st century.

This method of retrieving the vertical profile of O_3 using measurements of ultraviolet (UV) and visible solar radiation scattered from the earth's limb combines advantages of both the buv and the visible limb occultation methods. The geometry of the limb scatter measurement is shown in Figure 1, where the line-of-sight (LOS) of the instrument is pointed at the limb of the Earth just like the limb occultation method, and is denoted by the minimum height of the LOS above the Earth's surface or tangent height, TH. In the limb scatter case, however, the position of the sun is not restricted to be within the instrument field of view (FOV). This allows measurements to be made throughout the sunlit portion of the orbit as is done in the buv technique. Good vertical resolution (1-3 km) can be achieved by narrow angular viewing of the limb. In addition, the limb scatter method can be made nearly self-calibrating by using a normalization procedure similar to the limb occultation method.

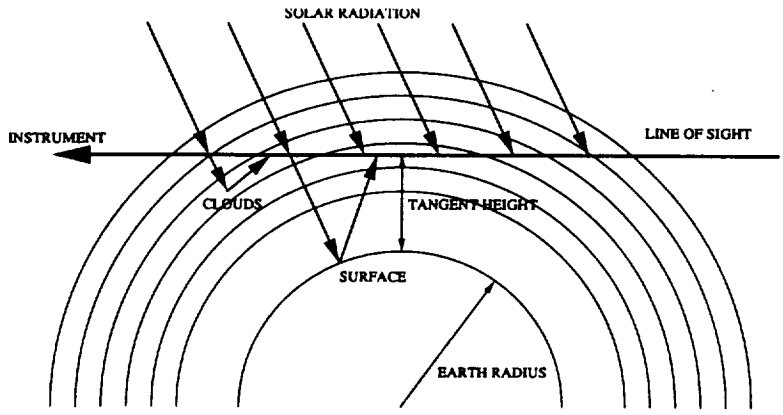

Figure 1: Geometry for limb scattering measurements.

The limb scatter technique has been demonstrated in the mesosphere (50-70 km) using UV data and single scattering theory [*Rusch et al.*, 1984]. Simulations showed that this method can be extended to the middle stratosphere using a multiple scattering model and wavelengths from 260 nm to 330 nm [*Aruga and Heath*, 1982]. However, probing the lower stratosphere with this technique requires that observations be made in the Chappuis band (near 600 nm) to decrease the molecular scattering optical depth [*Malchow and Whitney*, 1977; *Deepak & Wang*, 1983; *Herman et al.*, 1995a].

Here we present an algorithm for retrieving stratospheric O_3 profiles from measurements of UV and visible light scattered from the earth's limb. First the behavior of the limb radiance is given, then an O_3 retrieval algorithm is discussed including an analysis of the dominant error sources and the steps that can be taken to mitigate their effects. Results from applying this new method are presented in a companion article by *McPeters et al.* [this issue].

2. Forward Model Calculations

Simulated limb scattered radiance values, computed using a radiative transfer model that includes spherical geometry, all orders of scattering and polarization [*Herman et al.*, 1995b], are shown in Figure 2a. The form of the TH – radiance curve, or radiance profile, is controlled mainly by the vertical distribution of scatterers in the atmosphere. The radiance for a particular LOS is due to the scattering of light in the direction of the instrument FOV by scatterers all along the LOS (scattering into the LOS). This competes with the attenuation along the LOS by the scattering of light out of the LOS and extinction due to absorption (LOS attenuation). Illumination of the LOS is by two sources; the direct solar beam, typically from above, and by the diffuse light field (diffuse

illumination), mainly from below by the scattering of sun light off the surface of the earth and the atmosphere, including clouds.

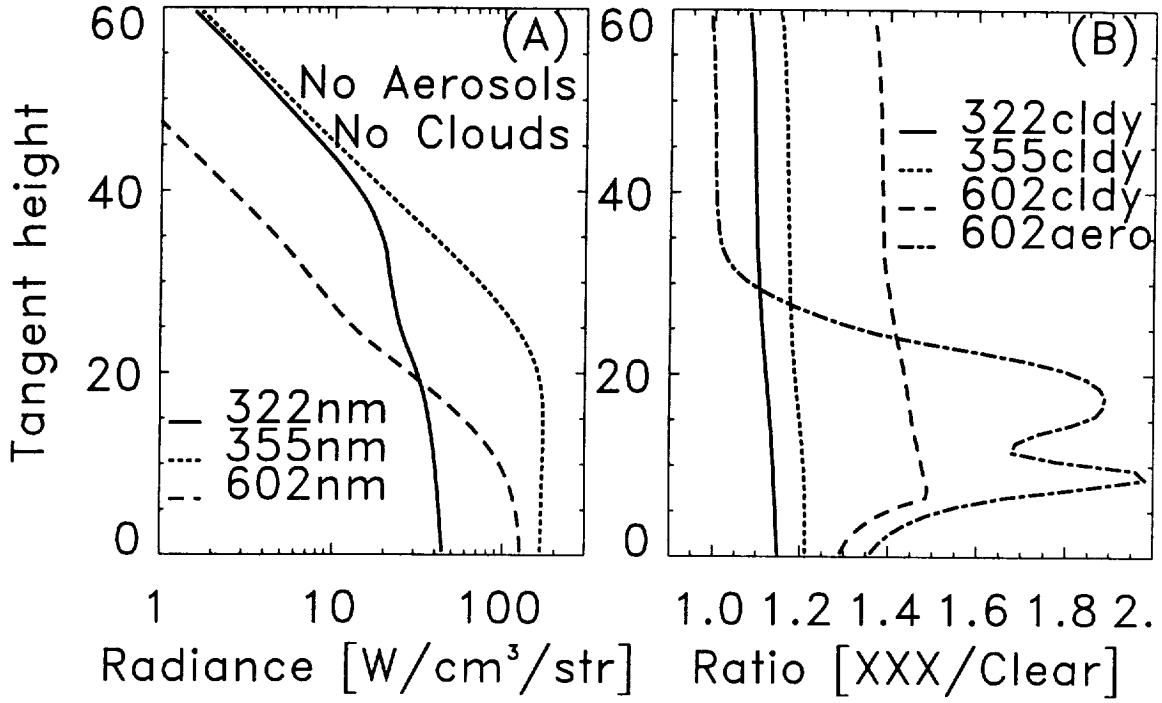

Figure 2: a) Simulated limb radiance profiles for a clear sky (no clouds or aerosols) atmosphere with a low-latitude O_3 profile (255 DU). b) Limb radiance for cases of a cloud at 8 km (cldy) and stratospheric aerosols (aero) relative to their clear sky counterparts in a).

Scattering into the LOS increases with decreasing TH due to the increase in molecular density with decreasing altitude, and hence the total number of scatterers along the LOS increases. This causes the radiance to also increase exponentially with decreasing TH. The increase continues until the LOS attenuation becomes large enough to cancel-out the additional scattering into the LOS. Below that height, the large attenuation along the LOS due to molecular scattering offsets the additional scattering into the LOS and the radiance changes rather slowly. When the optical depth along the LOS from the observer to the tangent point is small, <1, then the majority of the photons

seen by the observer had their last scattering event at or near the tangent point. As this optical depth increases, the mean region of last scattering moves along the LOS in Figure 1 from the tangent point toward the observer. For example, at 355 nm, for a TH=15 km, the LOS optical depth from the tangent point to space is 2.6 and the region of last scattering is actually centered between the tangent point and the observer at an altitude of 16.5 km.

Generally, the diffuse illumination is a factor for wavelengths > 300 nm. At 355 nm, the diffuse field can supply nearly half of the limb radiance, and is true even for a LOS which is optically thin, and thus has very few multiple scattering events along the LOS. For example, at 355 nm, a TH=50 km has a LOS optical depth from the tangent point to space of 0.0016, yet 30% of the limb radiance is due to the diffuse illumination even for an unrealistic surface reflectivity of 0.0. While the diffuse illumination contributes significantly to the limb radiance, all THs are affected in a similar manner. This is shown by the 'cldy' curves of Figure 2b. For a particular wavelength, nearly all the THs have the same sensitivity to the surface reflectivity.

Scattering of light by the stratospheric aerosol layer can also affect the limb radiance, especially when aerosols are within the FOV. The curve labeled '600aero' of Figure 2b shows the increase in the 600 nm radiance profile due to scattering by background stratospheric aerosols. The single scattering angle, 30°, of this case is relatively close to the forward direction, and thus this 80% increase in radiance can be thought of as a worst case situation under normal aerosol concentrations.

Sensitivity of the limb radiance to O_3 is shown in Figure 3. These plots illustrate the need to use both UV and visible wavelengths for profiling over the 15-60 km region. Attenuation by molecular scattering limits UV penetration such that wavelengths of 330 nm or longer have reduced sensitivity to O_3 without reaching lower altitudes. Making measurements at 600 nm greatly

reduces the molecular scattering optical depth, and allows one to probe the O_3 profile below 25 km. Using wavelengths longer than 600 nm only reduces the sensitivity to O_3 due to the decreased absorption cross-section, even though the molecular scattering optical depth is also less.

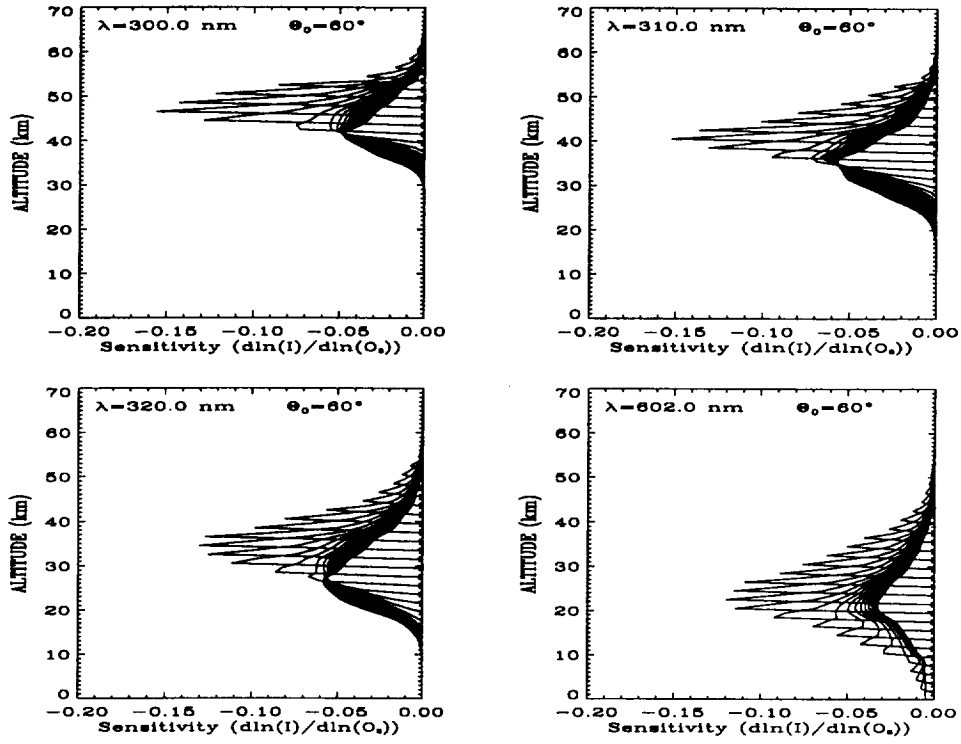

Figure 3: The fractional sensitivity, of the limb radiance change due to a change in the concentration of O_3 in discrete 1-km intervals, for a mid-latitude profile with 325 DU. Each curve is for a different tangent height from 0-70 (2) km.

3. Limb Scatter O_3 Retrieval Algorithm

This algorithm can be viewed as combining aspects of both the limb occultation method of O_3 profiling [*Chu et al.*, 1989] and the Total Ozone Mapping Spectrometer (TOMS) method of total O_3 estimation [*McPeters et al.*, 1998]. The fundamental measurement is limb radiance as a function of TH, or a radiance profile, at several wavelengths in the UV and visible regions of the spectrum. A basic set of wavelengths might include 300, 310, 322, 355, 525, 600, & 675 nm.

Shorter wavelengths can be used to extend the maximum altitude for this technique [*Rusch et al.* 1984]. This algorithm assumes that the attitude and pointing of the instrument is known, i.e. the value of TH for each LOS. If it is not known, *Janz et al.* [1996] showed that pointing could be obtained to better than 1 km accuracy using the shape of the 355 nm TH-radiance curve, which is dominated by molecular scattering.

3.1 Radiance Normalization

First of all, each limb radiance profile is normalized to the measured radiance at a reference altitude, typically a TH in the range of 60-45 km depending upon the wavelength and level of measurement noise. This normalization removes the need to measure the exoatmospheric solar irradiance and the absolute instrument calibration. These two characteristics are similar to the self-calibration feature of the limb occultation method where the unattenuated solar radiation is measured outside the atmosphere.

In addition, there is a reduction in the effect of the surface reflectance and clouds that can greatly control the diffuse illumination, even at high altitudes. For example, the limb radiance for 600 nm at TH = 20 km varies by 43% between a surface albedo of 0.0 and 0.8. However, when it is normalized to the radiance at TH = 55 km, the variation is reduced to 4.5% at 20 km and less for THs above this point. This normalized profile still contains information about the O_3 profile, since it is the absorption along the line of sight that produces the major portion of the signal for the retrieval of O_3.

3.2 Wavelength Pairs

To minimize the effect of aerosol scattering shown in Figure 2b, the ratio of two spectral channels is used in the retrieval. In the UV wavelengths with strong and weak absorption by O_3 are

paired together, similar to the TOMS method [*McPeters et al.*, 1998]. In the visible a triplet, $I_{600}/\exp(0.5(\ln(I_{525})+\ln(I_{675})))$, is used and is shown in Figure 4. Using this visible triplet of a strongly absorbing wavelength divide by the average of weaker absorbing wavelengths on either side still maintains the sensitivity to the O_3 profile, but greatly reduces the sensitivity to aerosols. The difference between the 'No Ozone' curve of Figure 4 (a non-absorbing molecular scattering case), and the other curves illustrates that the ratio is very sensitive to O_3. Additional curves are also shown for 'aged' aerosols and a cloud layer at 400 mb.

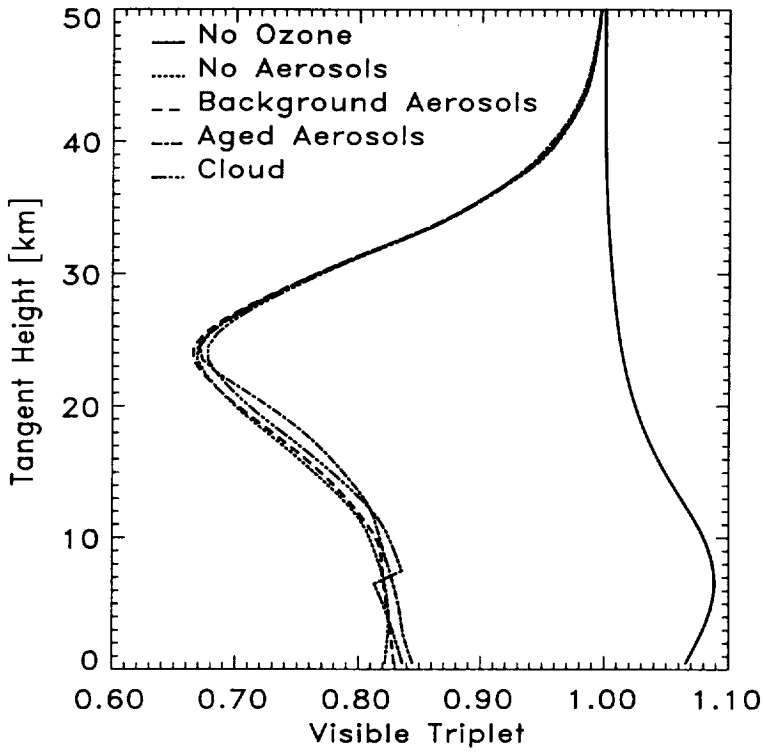

Figure 4: The visible triplet, shown for several atmospheric conditions, has a much smaller sensitivity to aerosols than does the radiances. The radiances are for conditions similar to Figure 2.

3.3 Optimal Estimation Retrieval

After the measured radiance profiles have been normalized and wavelengths paired together, forming y, they are combined with a climatological O_3 profile, x_0, in an optimal estimation scheme [*Rodgers*, 1976] to retrieve an O_3 profile, x_{n+1}. This is done in an iterative manner since the relationship between y and x is not strictly linear. This process can be written as,

$$x_{n+1} = x_0 + S^{-1} K_n^T S_e^{-1} (y - y_n - K_n (x_0 - x_n))$$

and

$$S^{-1} = (S_x^{-1} + K_n^T S_e^{-1} K_n)^{-1},$$

where y_n is the calculated y value using the radiative transfer model, K_n is the sensitivity of y_n to changes in x_n (i.e. from the family of curves in Figure 3), S_x is the covariance matrix of x_0, and S_e is the covariance matrix of the measurements y. Typically, only two to three iterations are required to obtain a change in the total column O_3 amount of less than 1%. It must be noted that only those measurements with a calculated LOS optical depth from the observer to the tangent point of less than 1.5, are used, and thus have the major contribution from scattering within the tangent layer.

3.4 Multiple Scatter Correction

In practice, the value of y_n is computed from model radiance calculations, which are in turn the sum of single scattering calculations for the profile x_n and multiple scatter corrections determined using a look-up table. The look-up table correction is a product of the single scatter for the profile x_n and the ratio of total scattered light to single scattered light interpolated from a pre-computed table using climatological O_3 profiles. This correction ratio is similar to that used in the buv method [*Bhartia et al.*, 1996] in that it is based mainly upon the total O_3 amount, which is a factor in the size of the upward diffuse radiation. Though the normalization procedure greatly reduces the

dependence upon the surface reflectivity, the wavelength dependence of a Lambertian equivalent reflectivity is computed by matching measured and calculated radiance values at non-absorbing channels. Measurements from tangent heights (30-35 km) are used for this average scene reflectivity, which is then used in the table interpolations.

3.5 Errors

The major error sources for this method are; instrument pointing, measurement noise, surface reflectance/clouds, and aerosol scattering. The estimated size of these errors is shown in Table 1 for the retrieval of a low latitude profile between 50 and 15 km with 2 km vertical resolution. In the upper stratosphere the pointing error is dominant since the concentration of O_3 changes so rapidly. Though the 1 km pointing error is larger than might be realized on some spacecraft, it is comparable to that experienced by SOLSE/LORE [*McPeters et al.*, this issue]. Errors caused by scattering from stratospheric aerosols are shown here as a worst case in that no aerosol scattering correction is used in the inversion and only the wavelength pairing is used. Additionally, they are for a scattering angle of 30° and decrease as this angle increases. Naturally, heavy aerosol loading from a large volcanic eruption like Pinatubo would render profiling retrieval impossible in the lower stratosphere.

Table 1: Analysis of Major Errors

	% Error in O_3 Density		
Type of Error	20 km	30 km	40 km
Pointing +/- 1km	30	5	20
Instrument Noise: 0.5 % (rms)	10	4	<4
Strat. Aerosols: Bkgd	5	1	<1
Strat. Aerosols: Aged	10	2	1
Clouds/Surface: +/- 100 mb	<1	<1	<1

4. Future Work

The use of an aerosol scattering correction scheme more sophisticated than the wavelength pairs and triplet used here is currently under development. One idea is to use limb measurements at a non-absorbing wavelength, such as 1μm, to obtain the relative concentration profile of aerosols [*Malchow and Whitney*, 1977; *Deepak and Wang*, 1983] and then use this information in the radiative transfer model. The merits of using more than three wavelengths in the visible for the aerosol correction are also being examined, with the possible result of using a more traditional Differential Optical Absorption Spectrometry (DOAS) [*Ferlemann et al.*, 1998] approach. Finally, the effects of horizontal variations in both the O_3 concentration and the surface reflectivity are being investigated and will be discussed in subsequent articles.

Acknowledgments. This research was supported by the NASA ACMAP grant #NAG5-7257.

References

Abrams, M.C., et al., Remote sensing of the Earth's atmosphere from space with high-resolution Fourier-transform spectroscopy, *Appl. Opt., 35*, 2774-2786, 1996.

Aruga, T. and D.F. Heath, Determination of vertical ozone distributions by spacecraft measurements using a limb-scan technique, *Appl. Opt., 21*, 3047-3054, 1982.

Bhartia, P.K., et al., Algorithm for the estimation of vertical ozone profile from the backscattered ultraviolet technique, *J. Geophys. Res., 101*, 18793-18806, 1996.

Bruhl, C., et al., Halogen Occultation Experiment ozone channel validation, *J. Geophys. Res., 101*, 10217-10240, 1996.

Chu, W.P., et al., SAGE II Inversion Algorithm, *J. Geophys. Res.*, *94*, 8339-8351, 1989.

Deepak, A., and P.-H. Wang, Retrieval of aerosol characteristics from scattering and extinction measurements, *Adv. Space Res.*, *2*, 55-64, 1983.

Ferelmann, F., et al., Stratospheric BrO profiles measured at different latitudes and seasons, *Geophys. Res. Lett.*, *25*, 3847-3850, 1998.

Froidevaux, L., et al., Validation of UARS Microwave Limb Sounder ozone measurements, *J. Geophys. Res.*, *101*, 10017-10060, 1996.

Herman, B.M., et al., A comparison of the Gauss-Seidel spherical polarized radiative transfer code with other radiative transfer codes, *Appl. Opt.*, *9*, 1760-1770, 1995a.

Herman, B.M., et al., Monitoring atmospheric ozone from space limb scatter measurements, *Proc. SPIE, Vol. 2583*, 88-99, 1995b.

Janz, S.J., et al., Rayleigh scattering attitude sensor, *Proc. SPIE, Vol. 2831-45*, 146-153, 1996.

Malchow, H.L. and C.K. Whitney, *Inversion of scattered radiance horizon profiles and gaseous concentrations and aerosol parameters* in *Inversion methods in atmospheric remote sensing* edited by A. Deepak, Academic Press, New York, pp. 217-261, 1977.

McPeters, R.D., et al., The retrieval of ozone profiles from limb scatter measurements: Results from the Shuttle Ozone Limb Sounding Experiment, *Geophys. Res. Lett., this issue*, 1999.

McPeters, R.D., et al., Earth Probe Total Ozone Mapping Spectrometer (TOMS) Data Product User's Guide, *NASA/TP-1998-206895*, 1998.

Remsberg, E.E et al., The validation of NIMBUS 7 LIMS measurements of ozone, *J. Geophys. Res.*, *89*, 5161-5178, 1984.

Rodgers, C.D., Retrieval of atmospheric temperature and composition from remote measurements of thermal radiation, *Rev. Geo. Sp. Phy.*, *14*, 609-624, 1976.

Rusch, D.W., et al., Solar mesosphere explorer ultraviolet spectrometer: measurements of ozone in the 1.0-0.1 mbar region, *J. Geophys. Res.*, *89*, 11677-11687, 1984.